nanomaterials

MDPI

Article

Cost Effective and Facile Fabrication of Tattoo Paper-Based SERS Substrates and its Application in Pesticides Sensing on Fruit Surfaces

Pratiksha P. Mandrekar [1], Mingu Kang [2], Inkyu Park [2], Bumjoo Kim [1,3] and Daejong Yang [1,3,*]

[1] Department of Future Convergence Engineering, Kongju National University, Cheonan 31080, Korea
[2] Department of Mechanical Engineering, Korea Advanced Institute of Science and Technology, Daejeon 34141, Korea
[3] Department of Mechanical and Automotive Engineering, Kongju National University, Cheonan 31080, Korea
* Correspondence: daejong@kongju.ac.kr

Abstract: Surface enhanced Raman spectroscopy (SERS) has been transformed into a useful analytical technique with significant advantages for sensitive and low concentration chemical analyses. However, SERS substrates are expensive and analyte sample preparation is complicated, hence it is being used in limited areas. We have fabricated tattoo paper-based SERS substrate by using non-complicated inkjet printing. The sensitivity of the SERS substrate was increased by removing carbon residues by exposing ultraviolet light without damaging of the substrate, and thus low concentrations of pesticides (upto 1-μM thiram) were measured. The SERS substrate was attached to a curved surface of the apple with the advantages like flexibility and easy attachability of tattoo paper and verified its feasibility by measuring 1-μM thiram on an apple surface. Due to its economic cost, simple usage and rapid measurement, it will be helpful not only for identification of agricultural adulterants yet also for food adulterants and water-based pollutant detection, also possibly for medical purposes related to human body surfaces in the future.

Keywords: flexible SERS substrates; Raman spectroscopy; silver nanoparticles; thiram; ultra violet light decomposition

1. Introduction

Today, when the world is growing at fast phase in terms of developments and technological advancements with a great amount of success, it is also seen that various factors affect the living beings on the planet like pollution, waste and other hazardous elements like pesticides and chemical adulterant as far as food industry is concerned. Human health considerably depends on the consumption of various food materials which are grown naturally and are agricultural products. These food materials are usually laced with various forms of pesticides and insecticides which are used for crop safety and growth, which often remains as a residue. Although the minute consumption of these products does not have any severe and immediate effect on living beings, long-term consumption can cause severe illnesses and harms [1-3]. Therefore, it is a requirement to develop a system that detects the harmful components in food materials and furthermore continuously monitoring them in culture and production processes.

In line with this trend, in this study, we present a facile and cost-effective way to measure pesticides on fruit surfaces. Gas chromatography (GC), liquid chromatography (LC), gas chromatography-mass spectrometry (GC/MS) and liquid chromatography-mass spectrometry (LC-MS) are used to analyze types and amounts of pesticide residues [4-8]. These methods separate an analyte into individual substances by using viscous force or

Citation: To be added by editorial staff during production.

Academic Editor: Firstname Lastname

Received: date
Revised: date
Accepted: date
Published: date

inertial force and then measure amounts of each substance. So, although this method is very precise and highly reliable, it requires very large or complicated components for the separation process. Therefore, these kinds of equipment are large and expensive, and take a long time for measurement, making them unsuitable for use in the field such as orchards. As an alternative, enzyme-linked immunosorbent assay (ELISA) has also been proposed, but it is also complicated and time-consuming [9-12]. For rapid and facile measurements, electrochemical or optical sensors using enzymes, aptamers, antibodies, cells, etc. are being widely developed [13-15]. However, these sensors also require pre-processes for the measurements, such as collecting samples and chopping them to extract analytes. Some methods collect analytes from the surface by rubbing or pressing a fruit surface. But these methods are also cumbersome and, due to poor repeatability, sampling itself reduces accuracy [16].

Therefore, a method for directly measuring pesticides on fruit surfaces needs to be developed. Surface-enhanced Raman spectroscopy (SERS) is based on molecular vibration as the signatures in the spectra, and electromagnetic amplification by conductive nanostructures [17-19]. Raman spectroscopy provides the specific information of the analyte as the fingerprint region of the molecule, thus providing information on the presence of the molecule [20]. Therefore, unlike conventional methods using enzymes, aptamers, antibodies or cells, various analytes can be measured without specifying the target in advance. However, since Raman signals are inherently weak, SERS which can achieve high sensitivity combined with electromagnetic amplification was developed [17-19,21,22]. Conductive NP clusters focus irradiated laser and generate high plasmonic hotspots that make SERS can detect even a single molecule [23-25]. Since it is based on electromagnetic amplification using conductive nanostructures, SERS devices are usually fabricated using sophisticated micro/nanostructure fabrication processes based on rigid substrates such as silicon and quartz [20,26,27]. Although extremely high sensitivity is achieved, they are designed to be suitable for measurement in laboratories and have limitations in application in work sites. Due to the high sensitivity of SERS, methods for detecting pesticides based on SERS have also been developed [28,29].

Even with SERS, sample collection processes are a fundamental drawback. Therefore, they have the same problems as chromatography, electrochemical, and optical sensing [28,29]. Methods for omitting analyte preparation processes need to be developed.

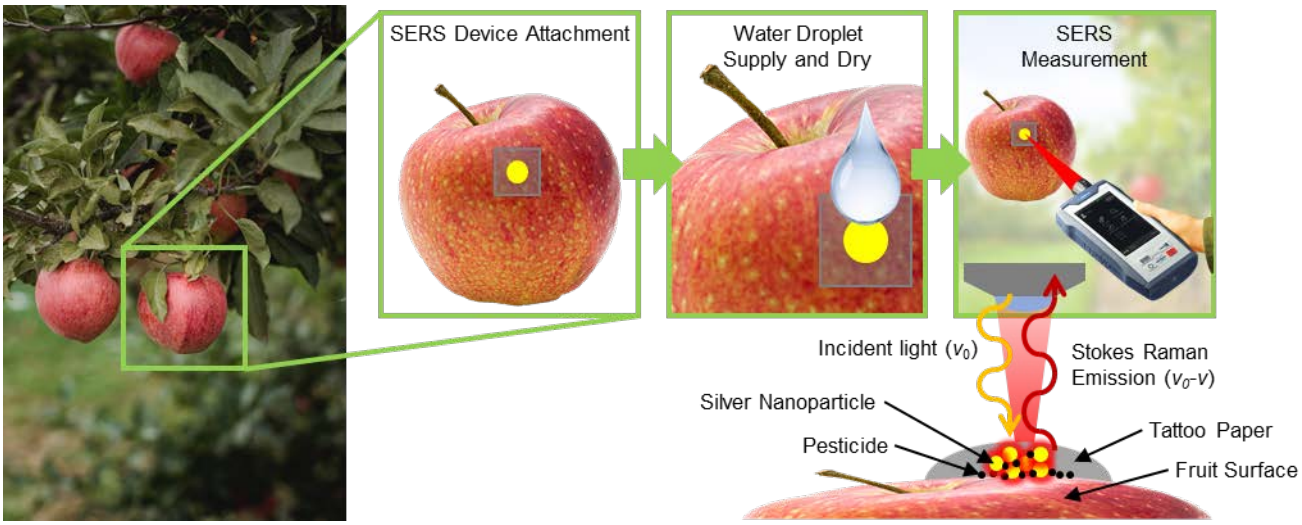

Figure 1. Application of the tattoo paper-based AgNPs SERS substrates on real fruit (apple) sample and identification of pesticide using the Raman spectrometer

Recently, high-performance SERS substrates using randomized high-density nanostructures have been developed, and they do not require sophisticated fabrication methods [30-32]. Since this type of device does not need to be limited to rigid substrates,

many flexible SERS substrates have been developed, thereby broadening the utilization of SERS [33-35]. Moreover, the production cost is also very low.

Various studies have been conducted in order to utilize flexible SERS substrates for the detection of various components on the fruit surfaces, but the majority of these methods involve pasting a substrate to the surface of the fruit and then peeling it off or rubbing and then peeling it off [36,37], which may often result in low accuracy detection of chemicals. Because they cannot guarantee the amounts of chemicals transferred to the SERS substrate from the fruit surface. Hence, to improvise these drawbacks and for easier attachment, we selected tattoo paper as a substrate, which just required to be attached to the surface of the fruit surface followed by direct detection on the surface itself. The schematic illustration in Figure 1 shows the application of this work. A piece of tattoo paper-based SERS substrate is attached to an apple in an orchard. Several drops of water used in the attachment process lead to close contact between silver nanoparticles (AgNPs) and pesticide molecules. The types and concentrations of pesticides on fruit surfaces are measured in real-time and in work sites using a portable Raman machine.

2. Materials and Methods

2.1 Chemical and Reagents

Chemicals and materials used in this work include silver ink (NBSIJ-MU01, Mitsubishi Paper Mills, Japan), ethanol (CH_3CH_2OH, 99% Daejung Chemicals & Metals Co., Ltd., Republic of Korea), benzenethiol (BT, C_6H_5SH, ≥99%, Sigma-Aldrich, USA), thiram ($C_6H_{12}N_2S_4$, PESTANAL®, analytical standard, Sigma-Aldrich, USA) and tattoo paper (Silhouette America, Inc., USA).

2.2 Fabrication of Tattoo Paper-Based AgNP SERS Substrates

AgNPs ink was printed on the tattoo paper by using an inkjet printer (Omni-100, Unijet, Republic of Korea). Figure 2 shows the fabrication procedure of tattoo paper-based AgNP SERS substrates. The protective layer of the tattoo paper was detached, and the carrier layer was directed downward so that the silver nanoparticle ink was printed on the upper adhesive layer. Patterns of AgNPs with a diameter of 2 mm at a spacing of 10 mm were printed. The AgNPs printed substrates were heated at 60 °C on a hotplate to ensure the complete drying of the ink on the tattoo paper. Since AgNPs ink contains organic solvents like ethylene glycol [38], it often results in the formation of carbon residue or carbon byproduct which tends to remain in the fabricated SERS substrates. In order to remove these carbon-based materials, substrates are usually heated over 300 °C, but at this high temperature, AgNPs may be agglomerated, and it is intrinsically impossible to apply that to this tattoo paper.

Instead of thermal decomposition, ultraviolet (UV) light decomposition process was employed to the tattoo paper-based AgNPs SERS substrates. A 254 nm wavelength UV light of 300 μW/cm² intensity generated by the 4 W lamp (TN-4LC, Korea Ace Sci., Republic of Korea) was irradiated to the SERS substrate for 60 hours.

After the carbon decomposition process, AgNPs patterns were diced to a size of 10 mm × 10 mm for convenient use.

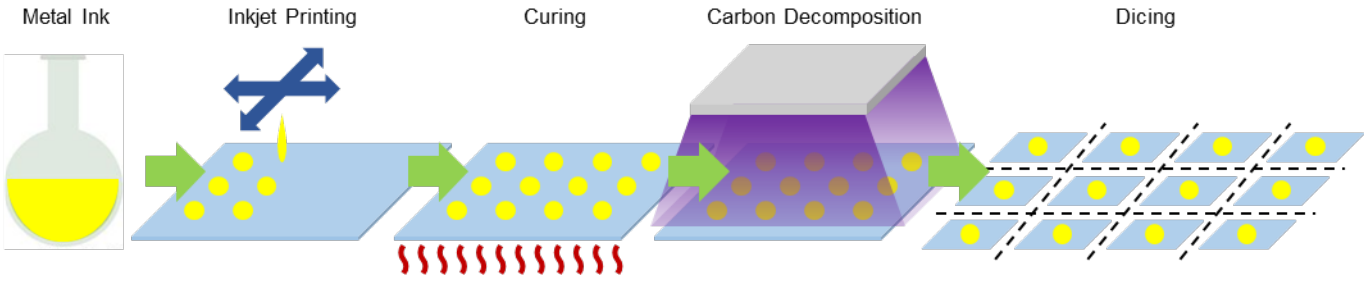

Figure 2. Fabrication steps of tattoo paper-based AgNP SERS substrates

2.3 Analysis of Tattoo Paper-Based AgNPs SERS Substrates

In order to verify the removal of residual carbon, SERS spectra were collected at randomly 10 points on the substrate after every 5 hours during 60 hours of the UV-light decomposition process. In addition, amounts of carbon before and after UV light irradiation were quantitatively measured using energy-dispersive X-ray spectroscopy (EDS). Due to the charging effect of the tattoo paper, glass substrate-based samples were fabricated for EDS.

The standard solutions of benzenethiol molar concentrations 1 μM and 1 mM were prepared using 99% ethanol as a diluent. The tattoo paper-based AgNP SERS substrates were incubated in the prepared solution for 24 hours and air-dried. Using a Raman spectrometer (XperRAM C Series, Nanobase Inc., Republic of Korea) with a 20× magnitude objective lens and 52.2 mW of 633 nm laser, the identifications of benzenethiol (1 μM and 1 mM concentrations) were carried out.

2.4 SERS Spectrum Measurement of Thiram

1, 10, 100, 200, 600 μM and 1 mM thiram standard solutions were prepared using 99% ethanol as a diluent. In the same manner as in benzenethiol, the SERS substrates were incubated in the thiram solution of six different concentrations and the SERS spectrum of each sample was measured.

2.5 SERS Spectrum Measurement of Thiram Using Real Fruit

The fresh Fuji apples from a grocery store were purchased, washed and cleaned thoroughly and repeatedly (4-5 times) using deionized water to ensure that any residual pesticides if present were completely removed. Once the apples were dried clean, they were subjected to high pressured jet air cleaning in order to eliminate any possible foreign residue or dust particles, creating a controlled experimental environment. These apples were then subjected to the solutions of thiram with concentrations of 1, 10, 100, 200, 600 μM and 1 mM individually. A piece of tattoo SERS sheet was placed on an apple and a small amount of water was supplied to wet the substrate. The carrier layer was removed, leaving only the tattoo layer on which AgNPs were printed, and the concentrations of thiram were measured by collecting SERS signals.

3. Results and Discussion

3.1. Characteristics of Tattoo Paper-Based AgNP SERS Substrates

The AgNP ink contains ethylene glycol to facilitate printing. The carbons in ethylene glycol have two main Raman peaks at 1320 cm^{-1} (the first-order D mode) and 1580 cm^{-1} (the first-order G mode) [39]. If a large amount of carbon residue remained, it overlaps with the main Raman peak of thiram which locates at 1382 cm^{-1} [40,41], preventing accurate measurement. In order to remove these carbon components, heating at a high temperature or immersing in an organic solvent are commonly used. However, the tattoo substrate used in this work cannot withstand high temperatures and harsh chemical atmospheres. In addition, not only the substrate can be damaged, but also AgNPs may be aggregated together or separated from the substrate, which will degrade the performance of the SERS substrate. So, we irradiated UV light which is another well-known method of decomposing carbon compounds [42-44]. Moreover, AgNPs used as SERS particles can also act as a catalyst for carbon decomposition [45,46]. UV lights were irradiated for a sufficiently long time (60 hours) to perfectly remove carbon residue. SERS signals were measured at 10 random points of the SERS substrate every 5 hours. Figure 3a shows the SERS spectrum of the substrates before and during 60 hours of UV light exposure. The carbon peaks at 1320 cm^{-1} and 1580 cm^{-1} were observed to be decreased dramatically, less than one-tenth, and the background signal was also greatly reduced. As shown in Figure 3b, a small amount of carbon remains after 40 hours of irradiation. Even so, in this work, the SERS substrates were irradiated for 60 hours to make reliable substrates. A 4 W UV

lamp was used and the temperature increase of the substrate during irradiation was neglectable, so using a high-power UV lamp would reduce the decomposition time. The decrease in carbon residue was indirectly proved by the intensity of the SERS signal, thus EDS was measured for quantitative verification. EDS data before and after 60 hours of UV light exposure also proved the decrease in carbon components (Figure 3c).

Figure 4a shows AgNP patterns on the tattoo substrate. It is printed with a 2 mm diameter and a spacing of 10 mm and diced into 10 mm × 10 mm cells for convent use. As shown in scanning electron microscope (SEM) images in Figures 4b, c and d, AgNPs were macroscopically uniformly coated on the tattoo paper, and microscopically rough surfaces of AgNPs clusters were observed. The size of each particle was measured using an image analysis program (ImageJ, National Institutes of Health, USA) and the average diameter was 19.5 nm and the standard deviation was 3.94 nm. These rough surfaces of the AgNP cluster concentrate electromagnetic field and amplify the Raman signal.

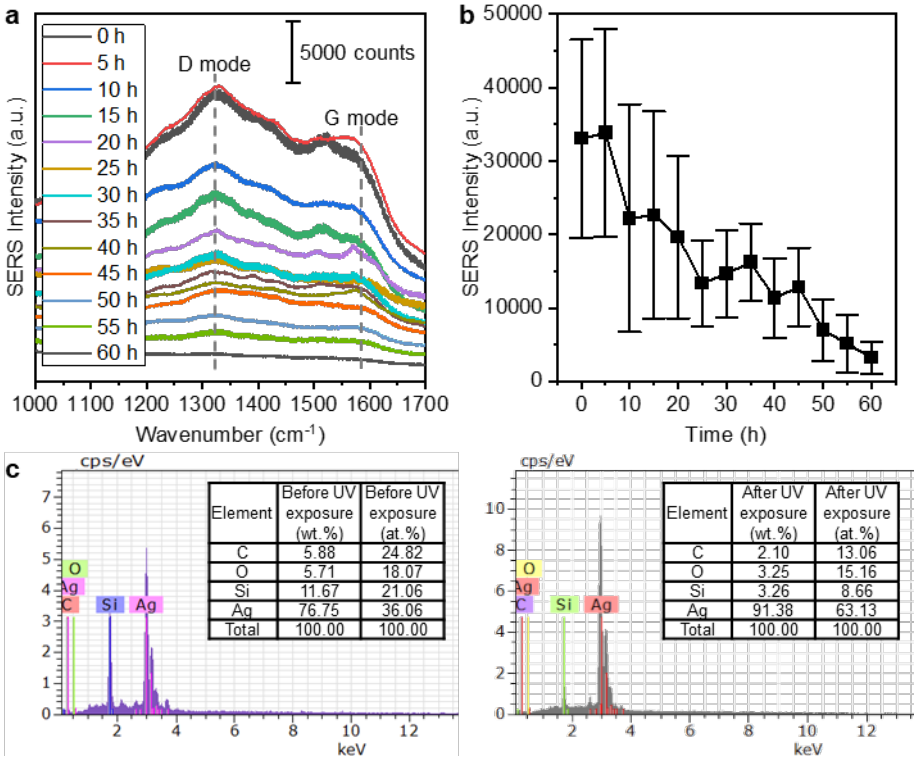

Figure 3. (a) SERS intensity spectra of substrates showing gradual carbon decomposition by UV irradiation, within the time period of 0 to 60 hours; (b) Reduction of carbon intensity during UV irradiation; (c) EDS data before and after the substrates being subjected to UV irradiation.

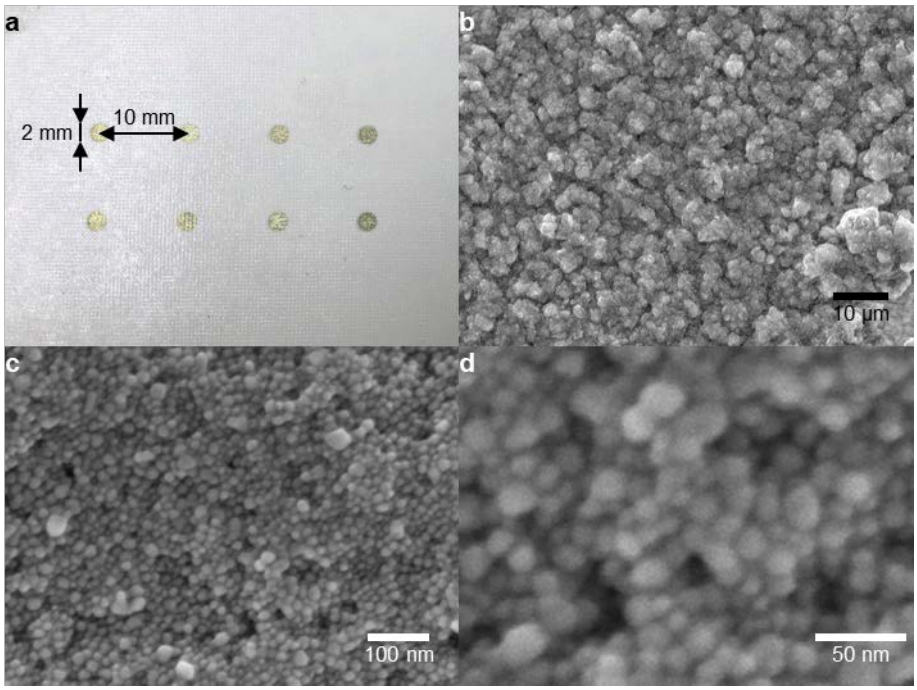

Figure 4. (a) Photo of printed AgNPs dot array on tattoo paper; (b, c, d) SEM images of the AgNPs clusters printed on the tattoo paper substrate.

3.2. Identification of Benzenethiol and Thiram

In order to evaluate the sensitivity of the tattoo paper-based SERS substrates, the diced substrates were incubated in 1 μM and 1 mM benzenethiol solutions. As shown in Figure 5a, five clear SERS peaks were observed from both 1 μM and 1 mM benzenethiol solutions. Four peaks came from benzenethiol and one came from tattoo paper. These peaks are located at 999 cm^{-1} (in-plain ring-breathing), 1022 cm^{-1} (in-plain C–H bending), 1072 cm^{-1} (C–S stretching), 1410 cm^{-1} (peak from the tattoo paper) and 1574 cm^{-1} (C–C stretching), and corresponded to main peaks of benzenethiol [31,47]. These large SERS picks prove that this tattoo paper-based substrates can be used as a SERS substrate for detecting chemicals.

The various concentrations of thiram solution were also measured in the same way as benzenethiol. Thiram can be identified with the SERS peaks located at 560 cm^{-1} (S–S stretching), 933 cm^{-1} (CH_3N stretching), 1144 cm^{-1} (C–N stretching and CH_3 rocking) and 1382 cm^{-1} (C–N stretching as well as symmetric CH_3 deformation) [40,41,48]. The strongest peak at 1382 cm^{-1} can be selected for the quantitative analysis. Figure 5b shows SERS the spectrum of 1, 10, 100, 200, 600 μM and 1 mM thiram solution. Small but clear peaks were observed at 560, 933 and 1144 cm^{-1}, and the largest and most clear peaks located at 1382 cm^{-1} were shown.

According to European Food Safety Authority (EFSA) [49], The acceptable daily intake and acute reference dose of thiram are 0.01 and 0.025 mg/kg/day, respectively. Assuming that a 70 kg person eats an apple with a diameter of 8 cm per day and that a 1 mm solution film is formed when a pesticide solution is sprayed in an orchard, the acceptable daily intake and acute reference dose of thiram are calculated as to 144.80 and 361.99 μM, respectively. Therefore, 1 μM to 1 mM of thiram solutions were used in this experiment.

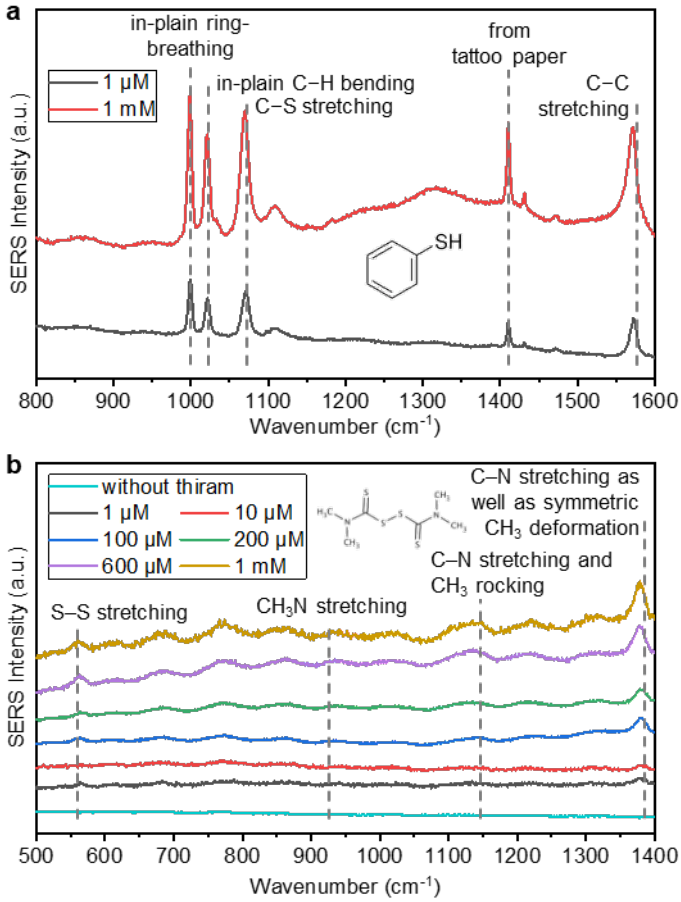

Figure 5. (a) SERS intensities at 999, 1022, 1072, 1410 and 1574 cm^{-1} which measured during the identification of 1 μM and 1 mM concentrations of benzenethiol solutions; (b) SERS intensities spectrum of without thiram and thiram with concentrations of 1, 10, 100, 200, 600 μM and 1 mM, exhibiting peak identification at 560, 933, 1144 and 1382 cm^{-1} for all the concentrations respectively.

3.3. Identification of Thiram Using Real Fruit

As a feasibility study, we measured thiram on a fruit surface. For reliable measurement, apples purchased from a grocery store were washed clean to remove pesticides or any other impurities on the surface. Various concentrations of thiram solutions were dropped on the surface of apples and dried to reproduce pesticide residues. Figures 6a and b show schematic illustrations and photos of measurement procedures. A piece of tattoo paper-based SERS sheet was placed on the surface of an apple and a few drops of water were dropped. The tattoo paper absorbed the water, and the carrier layer and the tattoo layer were gently separated. The AgNPs on the surface of the tattoo layer came into contact with the surface of the apple smeared by thiram, and the tattoo layer covered it. The water used to attach tattoo paper dissolves thiram molecules. This thiram dissolved solution is absorbed into the tattoo layer and it increases contact with the AgNPs layer. Since the tattoo layer has very high transparency, the laser can pass through it and reach the AgNPs. In addition, since the tattoo layer covers the SERS layer, the sensing layer can be protected from external friction that may be applied in an orchard.

Figure 6c shows the SERS spectrum of 1, 10, 100, 200, 600 μM and 1 mM thiram solution applied to apples. Four clear peaks at 560, 933, 1144 and 1382 cm^{-1} were observed. As shown in concentration-intensity curves in Figure 6d, the SERS intensity of the major three peaks increases as the concentration of thiram increases. This tattoo paper-based SERS substrate can detect 1 μM thiram on the surface of an apple by analyzing the clearest peak at 1382 cm^{-1}.

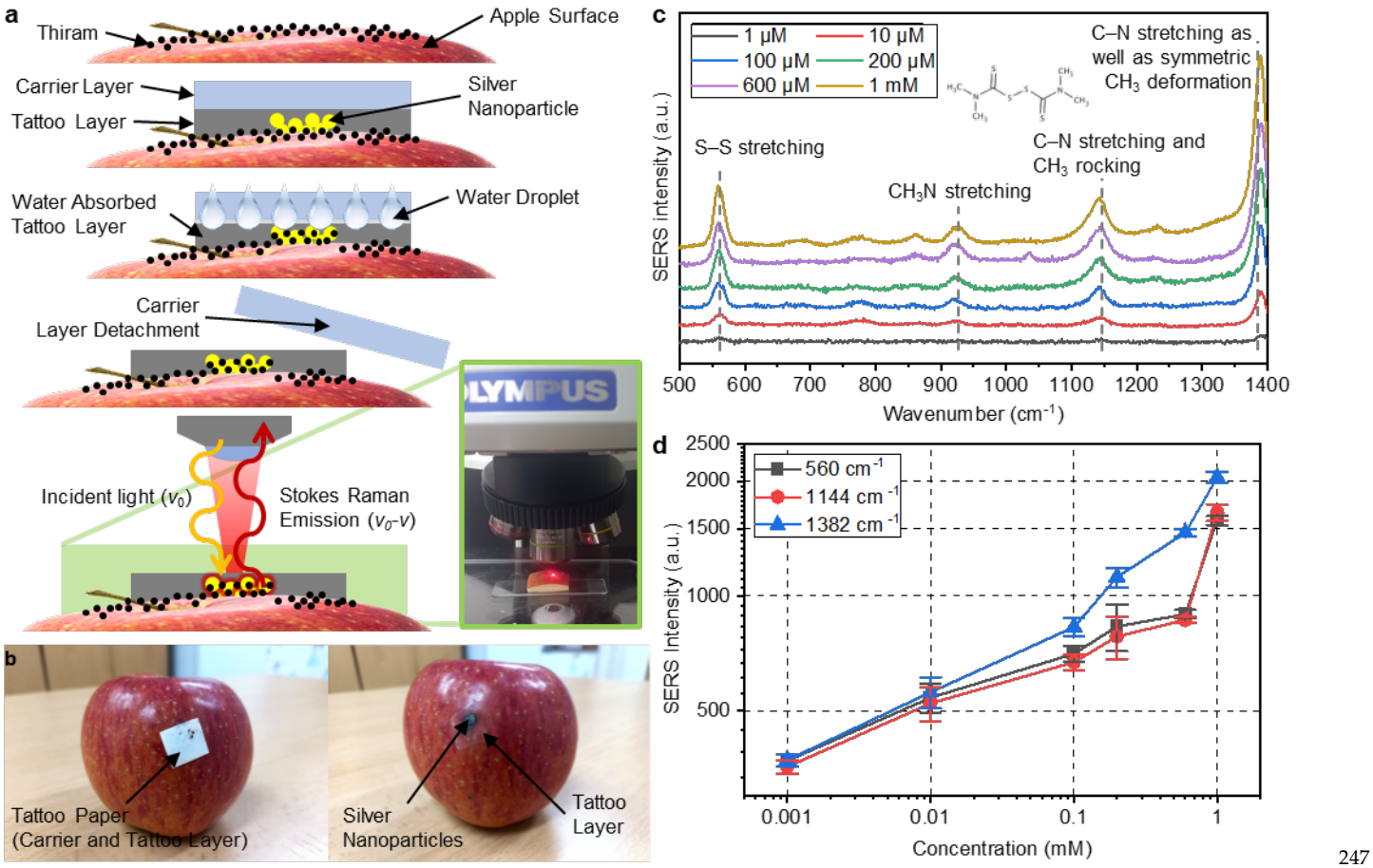

Figure 6. (a) Working mechanism of fabricated tattoo paper-based AgNP SERS substrates using thiram contaminated fruit (apple) sample; (b) Real apple specimen (thiram contaminated) used for the analysis; (c) SERS intensity spectrum of the apple specimen showing peak intensities at 560, 933, 1144 and 1382 cm^{-1} for the different concentration of 1, 10, 100, 200, 600 μM and 1 mM of thiram solutions; (d) Intensity curve showing increasing absorption at 560, 1144 and 1382 cm^{-1} peaks with the higher concentration level of thiram solutions.

4. Conclusions

In this study, we have fabricated tattoo paper-based AgNP SERS substrate. AgNPs were printed on the surface of tattoo paper using an inkjet printer. This method of utilizing an inkjet printer is not only helpful in speedy production, but it also enables the possibility of mass production. Moreover, it is fabricated at an ambient temperature and pressure, requires a very small quantity of ink, and inexpensive tattoo paper is utilized. Thus, it is a cost-effective technique. We ensured the sensing performance of the tattoo paper-based SERS substrate by measuring as low as 1 μM benzenethiol and thiram standard solution. To demonstrate the practicality, this substrate was applied to fruits. Tattoo paper being flexible and adhesive, was effortlessly attached to an apple surface. And it succeeded in detecting as low as 1 μM thiram on the apple surface. Further researches are needed to develop more sensitive SERS substrates for lower detection limits, to diversify detectable chemicals, and to elaborate quantification processes.

As this study presents a novel method of attaching SERS substrates onto curved surfaces, it can be used to analyze materials on the surface of various fruits and vegetables. Also, since the tattoo paper-based SERS substrates are considerably environment-friendly and cost-effective, and are very easy to handle and possess simpler sample collection methodology, they can be widely used for onsite pollutants detection in water and other

chemical-based food adulterants and additives for future works and applications. Furthermore, as tattoo paper can be easily attached on top of human and animal skin, it is expected to expand its use for medical purposes in near future.

Author Contributions: D.Y., P.P.M., M.K., I.P. and B.K. conceived and designed the experiments; P.P.M. and M.K. performed the experiments; D.Y. and P.P.M. analyzed the data; D.Y. and P.P.M. evaluated validation; D.Y. and P.P.M. wrote the article; D.Y., P.P.M., I.P. and B.K. reviewed the article. All authors have read and agreed to the published version of the manuscript.

Funding: This work was supported by the research grant of the Kongju National University in 2019.

Data Availability Statement: Data available in a publicly accessible repository.

Conflicts of Interest: The authors declare no conflict of interest.

References

1. Sivaperumal, P.; R.; Kumar, D.; Mehta, T.G.; Limbachiya, R. Human health risk assessment of pesticide residues in vegetable and fruit samples in Gujarat State, India. *Heliyon* **2022**, *8*, e10876.
2. Lerro, C.C.; Beane Freeman, L.E.; DellaValle, C.T.; Andreotti, G.; Hofmann, J.N.; Koutros, S.; Parks, C.G.; Shrestha, S.; Alavanja, M.C.R.; Blair, A.; Lubin, J.H.; Sandler, D.P.; Ward, M.H. Pesticide exposure and incident thyroid cancer among male pesticide applicators in agricultural health study. *Environ. Int.* **2021**, *146*, 106187.
3. Islam, M.A.; Amin, S.M.N.; Rahman, M.A.; Juraimi, A.S.; Uddin, M.K.; Brown, C.L.; Arshad, A. Chronic effects of organic pesticides on the aquatic environment and human health: A review. *Environ. Nanotechnol. Monit. Manag.* **2022**, *18*, 100740.
4. Alder, L.; Greulich, K.; Kempe, G.; Vieth, B. Residue analysis of 500 high priority pesticides: better by GC-MS or LC-MS/MS? *Mass. Spectrom. Rev.* **2006**, *25*, 838-865.
5. Khetagoudar, M.C.; Chetti, M.B.; Bilehal, D.C. Gas Chromatographic-Mass Spectrometric Detection of Pesticide Residues in Grapes. In *Gas Chromatography*; Peter Kusch, Ed.; IntechOpen: Rijeka, Republic of Croatia, 2019; Ch. 5, pp. 1–11.
6. Hogendoorn, E.A. High-Performance Liquid Chromatography Methods in Pesticide Residue Analysis. In *Encyclopedia of Analytical Chemistry*, 1st ed,; John Wiley & Sons, LTD.: New Jersey, United States, 2006; pp. 1–36.
7. Albero, B.; Sánchez-Brunete, C.; Tadeo, J.L. Determination of Thiabendazole in Orange Juice and Rind by Liquid Chromatography with Fluorescence Detection and Confirmation by Gas Chromatography/Mass Spectrometry After Extraction by Matrix Solid-Phase Dispersion. *J. AOAC Int.* **2019**, *87*, 664-670.
8. Ping, H.; Wang, B.; Li, C.; Li, Y.; Ha, X.; Jia, W.; Li, B.; Ma, Z. Potential health risk of pesticide residues in greenhouse vegetables under modern urban agriculture: A case study in Beijing, China. *J. Food Compos. Anal.* **2022**, *105*, 104222.
9. Nunes, G.S.; Toscano, I.A.; Barceló, D. Analysis of pesticides in food and environmental samples by enzyme-linked immunosorbent assays. *TrAC, Trends Anal. Chem.* **1998**, *17*, 79-87.
10. Wu, S.; Yan, C.; Fan, X.; Wang, H.; Wang, Y.; Peng, D. Development of enzyme-linked immunosorbent assay and colloidal gold-based immunochromatographic assay for the rapid detection of gentamicin in chicken muscle and milk. *Chinese J. Anal. Chem.* **2022**, *50*, 100142.
11. Huang, R.; Huang, Y.; Liu, H.; Guan, K.; Chen, A.; Zhao, X.; Wang, S.; Zhang, L. A bifunctional AuNP probe-based enzyme-linked immunosorbent assay for facile and ultrasensitive detection of trace zearalenone in coix seed. *Microchem. J.* **2023**, *184*, 108152.
12. Feng, R.; Wang, M.; Qian, J.; He, Q.; Zhang, M.; Zhang, J.; Zhao, H.; Wang, B. Monoclonal antibody-based enzyme-linked immunosorbent assay and lateral flow immunoassay for the rapid screening of paraquat in adulterated herbicides. *Microchem. J.* **2022**, *180*, 107644.
13. Pang, S.; Labuza, T.P.; He, L. Development of a single aptamer-based surface enhanced Raman scattering method for rapid detection of multiple pesticides. *Analyst* **2014**, *139*, 1895-1901.
14. Khadem, M.; Faridbod, F.; Norouzi, P.; Foroushani, A.R.; Ganjali, M.R.; Shahtaheri, S.J. Biomimetic electrochemical sensor based on molecularly imprinted polymer for dicloran pesticide determination in biological and environmental samples. *J. Iran. Chem. Soc.* **2016**, *13*, 2077-2084.
15. Moriwaki, H.; Yamada, K.; Nakanishi, H. Evaluation of the Interaction between Pesticides and a Cell Membrane Model by Surface Plasmon Resonance Spectroscopy Analysis. *J. Agric. Food Chem.* **2017**, *65*, 5390-5396.
16. Kumar, S.; Goel, P.; Singh, J.P. Flexible and robust SERS active substrates for conformal rapid detection of pesticide residues from fruits. *Sens. Actuators B Chem.* **2017**, *241*, 577-583.
17. Kahraman, M.; Mullen, E.R.; Korkmaz, A.; Wachsmann-Hogiu, S. Fundamentals and applications of SERS-based bioanalytical sensing. *Nanophotonics* **2017**, *6*, 831-852.
18. Pilot, R.; Signorini, R.; Durante, C.; Orian, L.; Bhamidipati, M.; Fabris, L. A Review on Surface-Enhanced Raman Scattering. *Biosensors* **2019**, *9*, 57.

19. Langer, J.; Jimenez de Aberasturi, D.; Aizpurua, J.; Alvarez-Puebla, R.; Auguié, B.; Baumberg, J.J.; Bazan, G.C.; Bell, S.E.J.; Boisen, A.; Brolo, A.G.; Choo, J.; Cialla-May, D.; Deckert, V.; Fabris, L.; Faulds, K.; García de Abajo, F.J.; Goodacre, R.; Graham, D.; Haes, A.J.; Haynes, C.L.; Huck, C.; Itoh, T.; Käll, M.; Kneipp, J.; Kotov, N.A.; Kuang, H.; Le Ru, E.C.; Lee, H.K.; Li, J.; Ling, X.Y.; Maier, S.A.; Mayerhöfer, T.; Moskovits, M.; Murakoshi, K.; Nam, J.; Nie, S.; Ozaki, Y.; Pastoriza-Santos, I.; Perez-Juste, J.; Popp, J.; Pucci, A.; Reich, S.; Ren, B.; Schatz, G.C.; Shegai, T.; Schlücker, S.; Tay, L.; Thomas, K.G.; Tian, Z.; Van Duyne, R.P.; Vo-Dinh, T.; Wang, Y.; Willets, K.A.; Xu, C.; Xu, H.; Xu, Y.; Yamamoto, Y.S.; Zhao, B.; Liz-Marzán, L.M. Present and Future of Surface-Enhanced Raman Scattering. *ACS Nano* **2020**, *14*, 28-117.
20. He, S.; Xie, W.; Fang, S.; Huang, X.; Zhou, D.; Zhang, Z.; Du, J.; Du, C.; Wang, D. Silver films coated inverted cone-shaped nanopore array anodic aluminum oxide membranes for SERS analysis of trace molecular orientation. *Appl. Surf. Sci.* **2019**, *488*, 707-713.
21. Liu, Y.; Wu, S.; Du, X.; Sun, J. Plasmonic Ag nanocube enhanced SERS biosensor for sensitive detection of oral cancer DNA based on nicking endonuclease signal amplification and heated electrode. *Sens. Actuators B Chem.* **2021**, *338*, 129854.
22. Mandavkar, R.; Lin, S.; Pandit, S.; Kulkarni, R.; Burse, S.; Habib, M.A.; Kunwar, S.; Lee, J. Hybrid SERS platform by adapting both chemical mechanism and electromagnetic mechanism enhancements: SERS of 4-ATP and CV by the mixture with GQDs on hybrid PdAg NPs. *Surf. Interfaces* **2022**, *33*, 102175
23. Moronshing, M.; Bhaskar, S.; Mondal, S.; Ramamurthy, S.S.; Subramaniam, C. Surface-enhanced Raman scattering platform operating over wide pH range with minimal chemical enhancement effects: Test case of tyrosine. *J. Raman Spectrosc.* **2019**, *50*, 826-836.
24. Bhaskar, S.; Thacharakkal, D.; Ramamurthy, S.S.; Subramaniam, C. Metal–Dielectric Interfacial Engineering with Mesoporous Nano-Carbon Florets for 1000-Fold Fluorescence Enhancements: Smartphone-Enabled Visual Detection of Perindopril Erbumine at a Single-molecular Level. *ACS Sustainable Chem. Eng.* **2023**, *11*, 78-91.
25. Parmigiani, M.; Albini, B.; Pellegrini, G.; Genovesi, M.; De Vita, L.; Pallavicini, P.; Dacarro, G.; Galinetto, P.; Taglietti, A. Surface-Enhanced Raman Spectroscopy Chips Based on Silver Coated Gold Nanostars. *Nanomaterials* **2022**, *12*, 3609.
26. Gao, T.; Xu, Z.; Fang, F.; Gao, W.; Zhang, Q.; Xu, X. High performance surface-enhanced Raman scattering substrates of Si-based Au film developed by focused ion beam nanofabrication. *Nanoscale Res. Lett.* **2012**, *7*, 399
27. Melekhov, E.; Penn, T.; Weidauer, T.; Abb, V.; Kammler, M.; Lechner, A. Tunable nanopillar array on a quartz-fiber tip for surface enhanced Raman scattering (SERS) detection. *Technisches Messen* **2022**, *89*, 70-81.
28. Chen, X.; Lin, M.; Sun, L.; Xu, T.; Lai, K.; Huang, M.; Lin, H. Detection and quantification of carbendazim in Oolong tea by surface-enhanced Raman spectroscopy and gold nanoparticle substrates. *Food Chem.* **2019**, *293*, 271-277.
29. Sitjar, J.; Liao, J.; Lee, H.; Liu, B.H.; Fu, W. SERS-Active Substrate with Collective Amplification Design for Trace Analysis of Pesticides. *Nanomaterials* **2019**, *9*, 664.
30. Calis, B.; Yilmaz, M. Fabrication of gold nanostructure decorated polystyrene hybrid nanosystems via poly(L-DOPA) and their applications in surface-enhanced Raman Spectroscopy (SERS), and catalytic activity. *Colloids Surf. A: Physicochem. Eng. Asp.* **2021**, *622*, 126654.
31. Yang, D.; Cho, H.; Koo, S.; Vaidyanathan, S.R.; Woo, K.; Yoon, Y.; Choo, H. Simple, Large-Scale Fabrication of Uniform Raman-Enhancing Substrate with Enhancement Saturation. *ACS Appl. Mater. Interfaces* **2017**, *9*, 19092-19101.
32. Izquierdo-Lorenzo, I.; Jradi, S.; Adam, P. Direct laser writing of random Au nanoparticle three-dimensional structures for highly reproducible micro-SERS measurements. *RSC Adv.* **2014**, *4*, 4128-4133.
33. Liu, S.; Tian, X.; Guo, J.; Kong, X.; Xu, L.; Yu, Q.; Wang, A.X. Multi-functional plasmonic fabrics: A flexible SERS substrate and anti-counterfeiting security labels with tunable encoding information. *Appl. Surf. Sci.* **2021**, *567*, 150861.
34. Chen, Y.; Ge, F.; Guang, S.; Cai, Z. Low-cost and large-scale flexible SERS-cotton fabric as a wipe substrate for surface trace analysis. *Appl. Surf. Sci.* **2018**, *436*, 111-116.
35. Lin, S.; Lin, X.; Han, S.; Liu, Y.; Hasi, W.; Wang, L. Flexible fabrication of a paper-fluidic SERS sensor coated with a monolayer of core–shell nanospheres for reliable quantitative SERS measurements. *Anal. Chim. Acta* **2020**, *1108*, 167-176.
36. Luo, J.; Wang, Z.; Li, Y.; Wang, C.; Sun, J.; Ye, W.; Wang, X.; Shao, B. Durable and flexible Ag-nanowire-embedded PDMS films for the recyclable swabbing detection of malachite green residue in fruits and fingerprints. *Sens. Actuators B Chem.* **2021**, *347*, 130602.
37. Zhang, S.; Xu, J.; Liu, Z.; Huang, Y.; Fu, R.; Jiang, S. Facile and scalable preparation of solution-processed succulent-like silver nanoflowers for 3D flexible nanocellulose-based SERS sensors. *Surf. and Interfaces* **2022**, *34*, 102391
38. Cai, Y.; Yao, X.; Piao, X.; Zhang, Z.; Nie, E.; Sun, Z. Inkjet printing of particle-free silver conductive ink with low sintering temperature on flexible substrates. *Chem. Phys. Lett.* **2019**, *737*, 136857.
39. Botti, S.; Rufoloni, A.; Rindzevicius, T.; Michael Stenbæk Schmidt. Surface-Enhanced Raman Spectroscopy Characterization of Pristine and Functionalized Carbon Nanotubes and Graphene. In *Raman Spectroscopy*; Gustavo Morari do Nascimento, Ed.; IntechOpen: Rijeka, Republic of Croatia, 2018; Ch. 10, pp. 203–219.
40. Pu, H.; Huang, Z.; Xu, F.; Sun, D. Two-dimensional self-assembled Au-Ag core-shell nanorods nanoarray for sensitive detection of thiram in apple using surface-enhanced Raman spectroscopy. *Food Chem.* **2021**, *343*, 128548.
41. Zheng, X.; Chen, Y.; Chen, Y.; Bi, N.; Qi, H.; Qin, M.; Song, D.; Zhang, H.; Tian, Y. High performance Au/Ag core/shell bipyramids for determination of thiram based on surface-enhanced Raman scattering. *J. Raman Spectrosc.* **2012**, *43*, 1374-1380.
42. Varadachari, C.; Mitra, S.; Ghosh, K. Photochemical oxidation of soil organic matter by sunlight. *Proc. Indian Natl. Sci. Acad.* **2017**, *83*, 223-229.

43. Böhnke, P.R.; Kruppke, I.; Hoffmann, D.; Richter, M.; Häntzsche, E.; Gereke, T.; Kruppke, B.; Cherif, C. Matrix Decomposition of Carbon-Fiber-Reinforced Plastics via the Activation of Semiconductors. *Materials* **2020**, *13*, 3267.
44. Austin, A.T.; Méndez, M.S.; Ballaré, C.L. Photodegradation alleviates the lignin bottleneck for carbon turnover in terrestrial ecosystems. *Proc. Natl. Acad. Sci. USA* **2016**, *113*, 4392-4397.
45. Ravikumar, S.; Mani, D.; Rizwan Khan, M.; Ahmad, N.; Gajalakshmi, P.; Surya, C.; Durairaj, S.; Pandiyan, V.; Ahn, Y. Effect of silver incorporation on the photocatalytic degradation of Reactive Red 120 using ZnS nanoparticles under UV and solar light irradiation. *Environ. Res.* **2022**, *209*, 112819.
46. Gola, D.; kriti, A.; Bhatt, N.; Bajpai, M.; Singh, A.; Arya, A.; Chauhan, N.; Srivastava, S.K.; Tyagi, P.K.; Agrawal, Y. Silver nanoparticles for enhanced dye degradation. *Current Research in Green and Sustainable Chemistry* **2021**, *4*, 100132.
47. Joo, T.H.; Kim, M.S.; Kim, K. Surface-enhanced Raman scattering of benzenethiol in silver sol. *J. Raman. Spectrosc.* **1987**, *18*, 57-60
48. Chen, J.; Huang, Y.; Kannan, P.; Zhang, L.; Lin, Z.; Zhang, J.; Chen, T.; Guo, L. Flexible and Adhesive Surface Enhance Raman Scattering Active Tape for Rapid Detection of Pesticide Residues in Fruits and Vegetables. *Anal. Chem.* **2016**, *88*, 2149-2155.
49. European Food Safety Authority, Peer review of the pesticide risk assessment of the active substance thiram. *EFSA Journal* **2017**, *15*, e04700.